



ON THE PHENOMENOLOGICAL ASPECT  
OF CREEP FRACTURE

\*  
MOHAMMED A. ABDOU

ABSTRACT

An inspection of experimental data obtained on ternary Nickel base alloy hardened by  $\gamma'$ -particles has shown that the dependence of the steady state creep rate,  $\dot{\epsilon}_s$ , on time to fracture,  $t_F$ , follows the correlation proposed by Milicka, taking the total deformation at fracture  $\epsilon_c$ , in account.

$$\log (t_F / \epsilon_c) + m \log \dot{\epsilon}_s = C$$

where  $m$  and  $C$  are constants.

The validity of this equation is verified. It indicates a close connection between strain accumulation and deformation mechanisms from start to fracture of the creep deformation process, and is a symptom of one process controlling strain during the whole test in spite of the different fracture mechanisms which can be observed.

INTRODUCTION

The request for structural materials for high temperature applications in recent years has led to an intensive worldwide research work devoted to the development of complex materials such as the various nickel-base alloys [1]. The high creep resistance of these alloys is usually obtained by a uniform dispersion of fine second phase particles which retard dislocation motion and by the precipitation of particles in the grain boundary which obstruct sliding. However the increase in creep strength is usually associated by a decrease in ductility of the material at high temperature [2], specially when the mode of failure is intergranular.

Monkman and Grant [3] have shown that, when the mode of failure is intergranular, the time to fracture dependence of the steady state creep rate can be described by the relationship :

$$\log t_F + m \log \dot{\epsilon}_s = C \quad \text{or} \quad |1|$$

\* Associate Professor, Mechanical Engineering Department,  
AL-Azhar University, Nasr City, Cairo, Egypt,

$$\dot{\epsilon}_s \cdot t_F = \text{constant, where}$$

$$t_F = \text{time to fracture}$$

m and C are constants.

The practical importance of this relation is considerable, for knowing the parameters m and C one can assess time to fracture on the basis of steady state creep rate. This can substantially shorten long time testing of the creep resistant materials, since the time to reach the steady state stage usually comprises only a small portion of time to fracture.

Less Scatter, in plots of  $t_F$  versus  $\dot{\epsilon}_s$ , has been obtained by Dobes and Milicka [4] taking the deformation at fracture,  $\epsilon_F$ , in account :

$$\log (t_F / \epsilon_F) + m' \log \dot{\epsilon}_s = C' \quad |2|$$

where m' and C' are constants and  $\epsilon_F$  is the true creep strain (defined as the difference between deformation at fracture and instantaneous deformation). The validity of this equation has been verified for several alloys [4].

Another important fundamental work on creep fracture, of polycrystalline copper containing a dispersion of Silica particles, has been carried out by Pavinchi and Raj [5].

$$\text{As } t_F \cdot \dot{\epsilon}_s = \text{constant}$$

$$\text{and } \dot{\epsilon}_s = A \sigma^n \quad |3|$$

the time to fracture can be expressed as :

$$t_F = A' \cdot \sigma^{-n'} \quad |4|$$

where  $n \approx n'$  and the constants A and A' depend on the temperature and microstructure of the material,  $\sigma$  is the applied stress.

The purpose of the present work was to (a) establish the relations between time to fracture  $t_F$  versus applied stress  $\sigma$  and steady state creep rate,  $\dot{\epsilon}_s$ , versus  $\sigma$  at temperature of 1023 K. For Nickel-22 at % Cobalt-13 at % Aluminium alloy. (b) identify the fracture mode for the alloy at different stresses. (c) compare the present results with those previously obtained [6], at 1073 K, for the same batch of material in order to check the validity of Milicka's equation which relate time to fracture and steady state creep rate to the total creep deformation

EXPERIMENTAL PROCEDURE

Nickel -22 at % Cobalt -13 at % AL hardened by  $\gamma'$ - particles was creep tested at 1023 °K. The alloy was solution treated for ½ hr at 1343 K in vaccum followed by water quenching. Ageing at 1023 K produced a uniform distribution of Cuboid  $\gamma'$  - particles in the matrix. The alloy was aged for 15 hr prior to the creep test.

Constant stress creep tests were performed in air at the ageing temperature. Stresses were varied from  $\approx 95-185 \text{ MN/m}^2$ . These conditions created

fracture times ranging from approximately  $3.4 \times 10^{-9}$  to  $8.56 \times 10^{-8}$  seconds. The specimen extension was measured by means of differential-capacitive transducers capable of reading to  $1 \times 10^{-5}$  mm. The specimen temperature was maintained to  $\pm \frac{1}{2}$  K. After conducting the test each specimen was then sectioned, electropolished, and inspected by both optical and scanning microscopy to determine the mode of fracture.

### RESULTS

Metallographic observations have shown that cavitation is the favoured mode of intergranular fracture at low strain rates ( $\dot{\epsilon}_s < 15 \times 10^{-8}/s$ ). At strain rates higher than  $15 \times 10^{-8}/s$ , fracture occurred by triple point cracking.

Typical creep curves are shown in Fig.(1). At temperature of 1023 k, the time spent in primary and tertiary creep was small compared to the fracture life. However, comparing the present results with those previously obtained, at 1073 k, it is clear that both of the strain and time in tertiary stage are comparable with those of strain and time to fracture.

Fig.2 shows log-log plot of  $\dot{\epsilon}_s V_s \sigma$  and  $t_F V_s \sigma$  at two different temperatures. The results are accurately described by equation (3) and (4). The agreement between  $n$  and  $n'$  is evidently clear, representative results, illustrating, stress range, strain rate range and time to fracture range are given in table 1.

The ductility,  $\epsilon_F$ , defined as the product of time to fracture,  $t_F$ , and steady state creep rate  $\dot{\epsilon}_s$  was found to depend strongly on the test temperature and consequently on the volume fraction and dispersion of  $\gamma'(Ni_3Al)$ . At temperature of 1023 k the ductility values were very small (see table.1).

Table 1. Experimental values of creep and fracture parameters at 1023 k.

Stress, $\sigma$ MN/m <sup>2</sup>	Creep rate $\dot{\epsilon}_s$ S <sup>-1</sup> x 10 <sup>8</sup>	Ductility $\epsilon_F \times 10^3$	Time to fracture $t_F, S$	$T_F / \epsilon_F$ x 10 <sup>-3</sup>
97.3	0.34	0.975	142920	146584
120	0.70	1.000	72720	72720
136.2	1.29	0.517	48600	44003
148.9	2.02	1.180	27972	23705
160	3.13	0.930	14400	15483
184	8.56	0.865	5076	5868

It should be, also, pointed out that the above definition of ductility describe the results accurately at 1023 k where the difference between the actual ductility as measured by the capacitive transducers and  $\epsilon_F$  was equal to the strain accumulated during primary creep which was always small compared to the total strain to fracture. However, at 1073 k, the total strains to fracture were large compared to those observed during primary and steady state creep stage Fig.1. Therefore it is more appropriate to define the ductility as the difference between deformation at fracture and the instantaneous deformation.

The dependence of time to fracture on steady state creep rate is shown in Fig.3. The results could be accurately described by equation (3).

$$\log t_F + m \log \dot{\epsilon}_s = C$$

The values of  $m$  is approximately equal to unity and  $C$  is temperature dependant. Further inspection of the results Fig.4, has shown that the dependence of time to fracture on the steady state creep rate is more accurately described by equation (4) as :

$$\log (t_F/\epsilon_F) + m' \log \dot{\epsilon}_s = C'$$

where  $\epsilon_F$  is the total creep strain defined as above and  $m' \approx 0.9$ .

#### DISCUSSION

It is usually considered that the relation between creep rate and time to fracture could be used as a useful guide to identify the possible fracture mechanism. In the present case, the product  $\dot{\epsilon}_s t_F$  is constant for constant temperature and microstructure Fig.3. This relationship was shown [7] to be valid when alloys fail by the cavitation mechanism. However, the range of applicability of the described relation would also suggest that it also applies for triple-point cracking mechanism [8] as it is observed at high strain rates. The present results, Fig.4, also indicate that there is a definite relationship between the actual creep strain and the deformation process irrespective of the different fracture mechanisms which can be observed as suggested by Milicka [4].

Cavities were found to nucleate at the grain boundaries before the onset of steady state creep. This was probably due to grain boundary sliding [9] or as a result of grain boundary precipitates [10]. Nucleation is followed by cavity growth either by diffusional transport of vacancies via the grain boundaries or lattice diffusion [11] or as a result of grain boundary sliding [12] or matrix deformation [5]. In the present case, the measured failure times were compared with those estimated for diffusional growth of cavities [11]. The predicted times to fracture were always much shorter than those experimentally observed. However, in the range of strain rates and temperatures used in this work, there was a strong evidence of matrix deformation to be the dominant cavity growth mechanism as indicated by the rate equations for time to fracture and steady state creep rate.

$$\begin{aligned} \text{Since } t_F &= A' \sigma^{-n'} \\ \text{and } \dot{\epsilon}_s &= A \sigma^n \end{aligned}$$

It is undoubtedly clear from Fig.2 that both of time to fracture and steady state creep rate, have similar dependence on the applied stress.

#### CONCLUSIONS

1. In ternary Ni/Co/AL alloy creep fractured at high temperatures, the product of steady state creep rate and time to fracture is proportional to the total creep deformation.
2. At low creep rates, fracture occurred as a result of growth and

6  
 coalescence of cavities whereas at high creep rates fracture was due to growth of triple point cracks.

3. The time to fracture and steady state creep rate have similar dependence on the applied stress indicating a close connection between deformation process and processes leading to the formation of cavities and cracks and eventually to fracture.

#### REFERENCES

1. Coustouradis, D. and Felix, P., "High Temperature Alloys for Gas Turbines" Applied Science Publishers. London (1978).
2. Ashby M.F., Gandhi C., and Taplin D.M.R., "Fracture Mechanism Maps and their construction", Acta Metall., 27, 699-728, (1979).
3. Monkman F.C., and Grant, "An empirical relationship between rupture life and minimum creep rate in creep rupture tests", ASTM, 56, 593-605 (1956).
4. Dobes, F., and Milicka K., "The relation between minimum creep rate and time to fracture", J. Metal science, Nov., 382-384 (1976).
5. Pavinchi W., and Ray R., "Fracture at Elevated temperature", Metall. Transactions, 8A Dec., 1917, 1933 (1977).
6. Abdou M.A., "Creep of Ni-base alloys", Ph.D. Thesis. London University, England, (1977).
7. Davies, P.W.D and Wilshire B., "Structural Processes in creep", The Iron and Steel institute, London, 101, (1961).
8. Williams J.A., "A theoretical derivation of the creep life of commercial materials failing by triple point cracking", Philos. Mag., 15, 1289-1291, (1967).
9. Mclean D., "A Note on the Metallography of Cracking during creep", J. Inst. of metals, 85, 468-473, (1956-1957).
10. Weaver C.W., "Intergranular Cavitation, structure, and creep of a Nimonic 80A-Type Alloy", J. Inst of metals, 88, 296-300, (1959-1960).
11. Hull D., and Rimmer D.E., "The growth of Grain boundary voids under stress", Philos. Mag., 4, 673, 1959.
12. Davies P.W. and Williams K.R., "Cavity growth by grain-boundary sliding during creep", J. Metal science, 3, 220-225, (1969).

#### ACKNOWLEDGEMENT

The author wishes to thank Prof. M.A. Rifai for useful discussion and use of metallographic facilities. The assistance of Eng. Adel Abdel Moneim in preparing the final form of the manuscript is also appreciated.

#### NOMENCLATURE

- A, A', C, C', m, m' and n, n' constants  
 $t_F$  time to fracture  
 $\dot{\epsilon}_S$  steady state creep rate  
 $\sigma^S$  applied stress

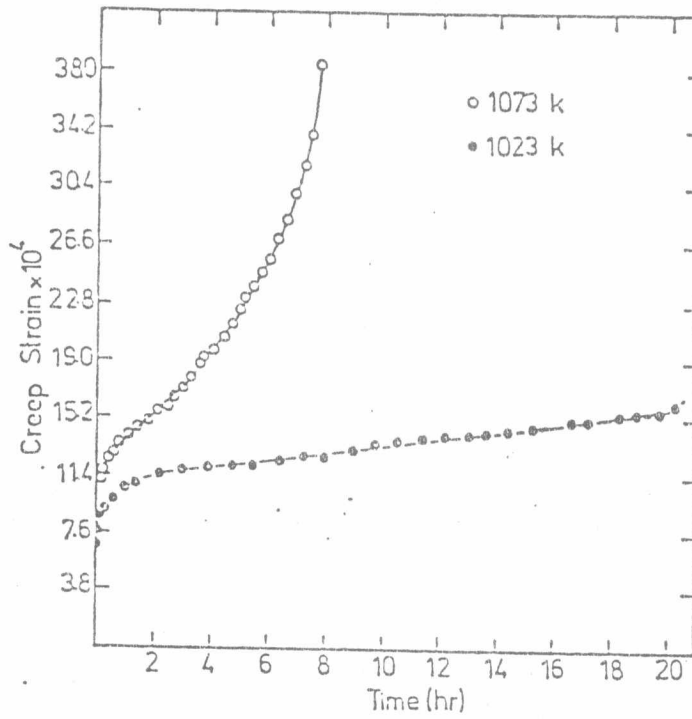


Fig.1 Typical creep curves. ( $\sigma = 120 \text{ MN/m}^2$ )

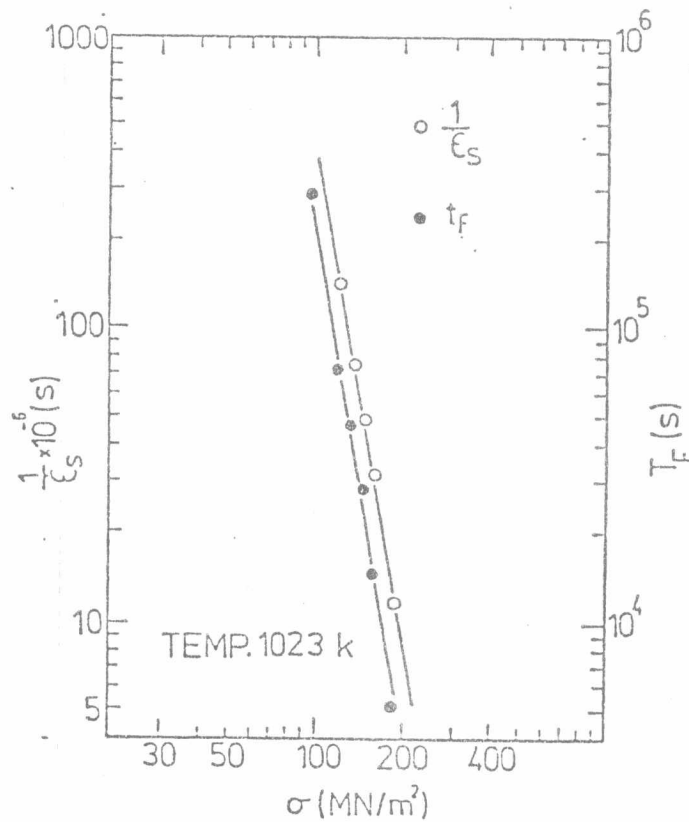


Fig.2(a) Typical curve  $\dot{\epsilon}_s^{-1}$  and  $T_F$  vs  $\sigma$  at 1023K.

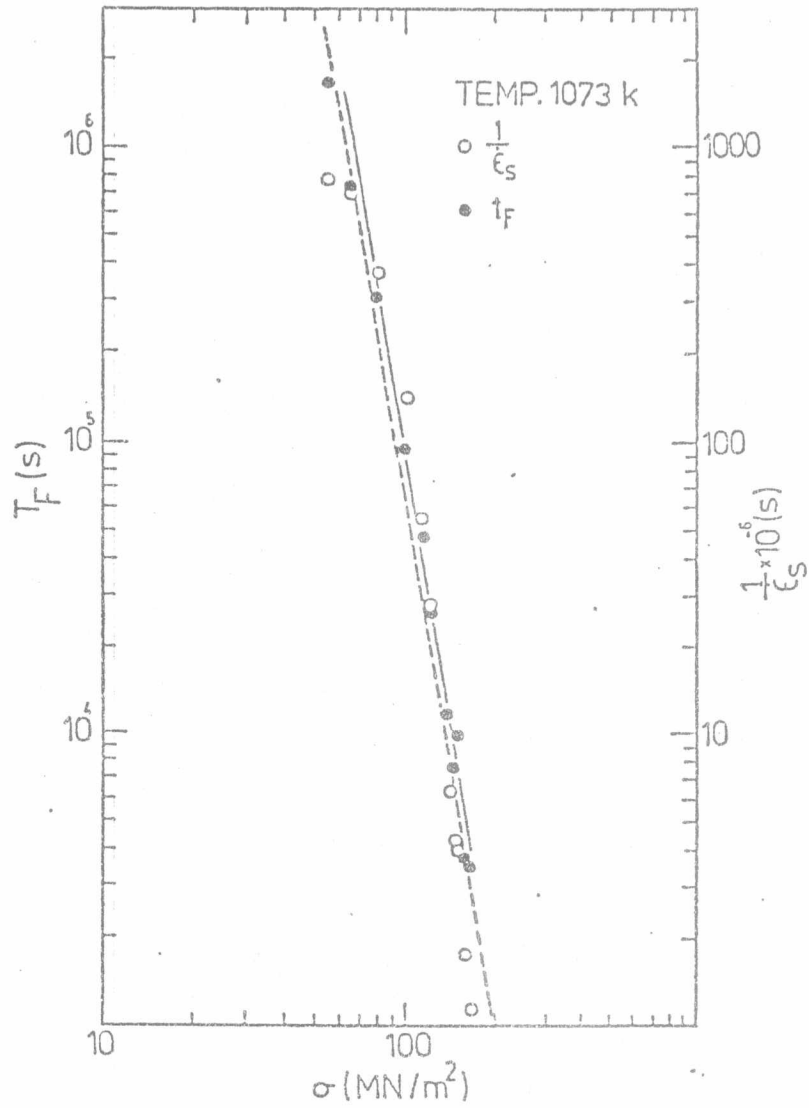


Fig.2(b) Typical curve  $\dot{\epsilon}_s^{-1}$  and  $T_F$  vs  $\sigma$  at 1073K.

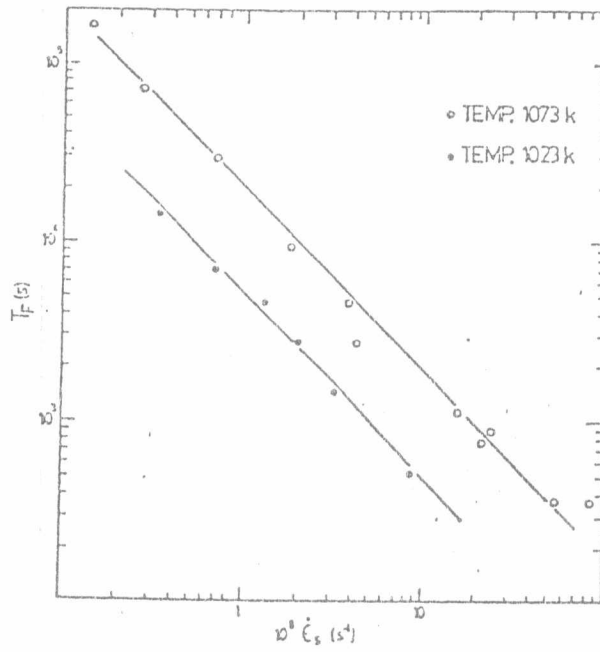


Fig.3 Dependence of time to fracture  $t_f$  on steady state creep rate.

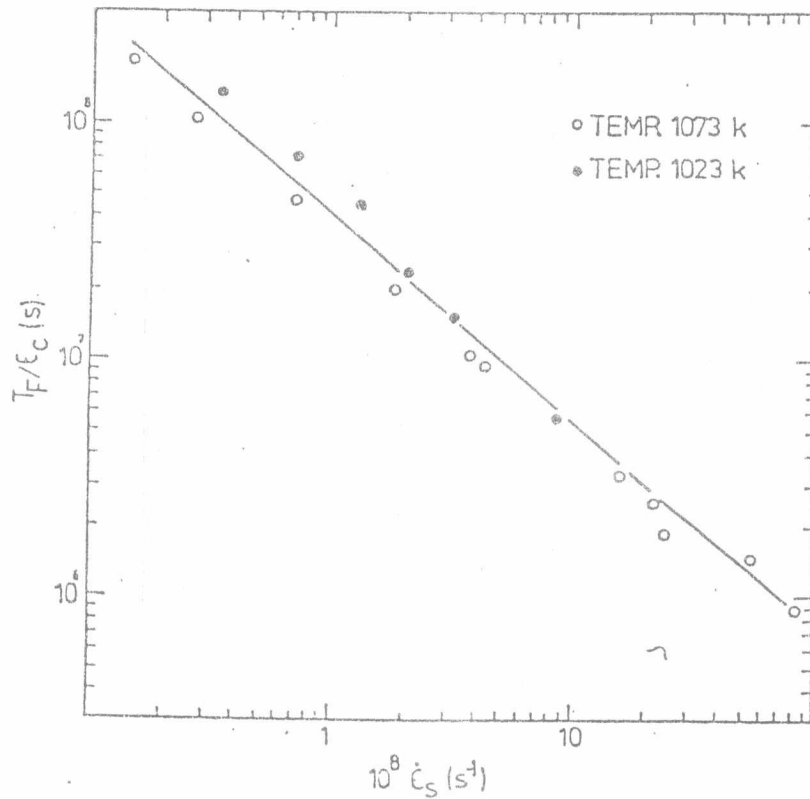


Fig.4 Dependence of ratio of time to fracture  $t_f$  to total creep deformation  $\epsilon_f$  on steady state creep rate  $\dot{\epsilon}_s$ .